Structure-Variant Exciton Transfer and Spatial Confinement in Statistical Copolymers and Blends Based on Polybenzazoles

Zitao Liu,[†] Shanfeng Wang,*[,‡] Qixin Zhuang,*[,†] Xinxin Li,[†] Fuyou Li,[§] Pingping Wu,[†] and Zhewen Han[†]

Key Laboratory for Ultrafine Materials of Ministry of Education, School of Materials Science and Engineering, East China University of Science and Technology, Shanghai 200237, People's Republic of China, Departments of Orthopedic Surgery and Biomedical Engineering, Mayo Clinic, Rochester, Minnesota 55901, and Department of Chemistry, Fudan University, Shanghai 200433, People's Republic of China

Received September 10, 2006. Revised Manuscript Received December 19, 2006

In an effort to explore the applications of polybenzazoles with extraordinary mechanical properties, thermal stability, and electron transport properties, a series of copolymers and blends consisting of a higher band gap poly(2,5-benzoxazole) (ABPBO) and a lower band gap poly(2,5-thienyl benzobisthiazole) (PBZTT) with different PBZTT compositions were synthesized and characterized. Structure-variant mechanisms of both exciton transfer and spatial confinement were revealed in tuning emitting color and efficiency using these statistical copolymers and blends. The absorption and emission maxima could be well modulated by the composition of PBZTT in both copolymers and blends; however, the composition dependence of emission maxima was significantly different, and only copolymers showed enhanced quantum efficiencies as high as 14 times compared to PBZTT. This difference was interpreted using a schematic illustration of composition-dependent supramolecular structures in both copolymers and blends.

Introduction

Conjugated polymers can be readily tailored to realize desired emitting properties in polymeric light emitting diodes.[1,2] Among them, heterocyclic rigid-rod polybenzazoles such as poly(*p*-phenylene benzobisoxazole) (PBO) have exhibited efficient electron transport and third-order nonlinear optical properties as well as their well-known outstanding mechanical properties and excellent thermal and environmental stability.[3−7] Like other conjugated polymers, polybenzazoles in the solid state suffer from low quantum efficiency because of the formation of excimer and/or aggregate.[4a,5a] Although quantum efficiency can be enhanced by decreasing interchain interaction through blending or attaching alkyl chain substituents onto the polymer backbone, these two methods have shortcomings such as phase separation in polymer blends and dilution of the active chromophore upon substitution, which consequently deteriorate charge transport.[1,2,8] Thereby, incorporating low-energy segments in the polymer backbone via random copolymerization is of current interest because it can efficiently enhance quantum efficiency and tune emission wavelength for full-color displays based on energy transfer principle.[9]

Previously, Chen and Jenekhe made semiconducting polymer quantum wires from the triblock copolymer poly(2,5-benzoxazole)-*b*-poly(*p*-phenylene benzobisthiazole)-*b*-poly(2,5-benzoxazole) (ABPBO-*b*-PBZT-*b*-ABPBO) with a band gap difference ΔE_g of 0.76 eV between ABPBO (E_g = 3.24 eV) and PBZT (E_g = 2.48 eV).[10] We also reported a series of random copolymers consisting of PBO (E_g = 2.79 eV) and ABPBO or poly(2,5-thienyl benzobisoxazole) (PBOT) (E_g = 2.47 eV).[5a,c] In this study, statistical, random

* To whom correspondence should be addressed. Tel.: 507-538-1667. Fax: 507-284-5075. E-mail: wang.shanfeng@mayo.edu; qxzhuang@ecust.edu.cn.
† East China University of Science and Technology.
‡ Mayo Clinic.
§ Fudan University.

(1) Kraft, A.; Grimsdale, A. C.; Holmes, A. B. *Angew. Chem., Int. Ed.* **1998**, *37*, 403.
(2) Kim, D. Y.; Cho, H. N.; Kim, C. Y. *Prog. Polym. Sci.* **2000**, *25*, 1089.
(3) (a) Wolfe, J. F. In *Encyclopedia of Polymer, Science, and Technology*, 2nd ed.; Mark, H. F., Kroschmitz, J. I., Eds; Wiley: New York, 1988; Vol. 11, pp 601−635. (b) Wolfe, J. F.; Loo, B. H.; Arnold, F. E. *Macromolecules* **1981**, *14*, 915.
(4) (a) Jenekhe, S. A.; Osaheni, J. A. *Science* **1994**, *265*, 765. (b) Osaheni, J. A.; Jenekhe, S. A. *J. Am. Chem. Soc.* **1995**, *117*, 7389. (c) Osaheni, J. A.; Jenekhe, S. A. *Chem. Mater.* **1992**, *4*, 1282. (d) Alam, M. M.; Jenekhe, S. A. *Chem. Mater.* **2002**, *14*, 4775. (e) Babel, A.; Jenekhe, S. A. *J. Phys. Chem. B* **2002**, *106*, 6129. (f) Kulkarni, A. P.; Tonzola, C. J.; Babel, A.; Jenekhe, S. A. *Chem. Mater.* **2004**, *16*, 4556.
(5) (a) Wang, S.; Wu, P.; Han, Z. *Macromolecules* **2003**, *12*, 4567. (b) Wang, S.; Guo, P.; Wu, P.; Han, Z. *Macromolecules* **2004**, *37*, 3815. (c) Chen, Y.; Wang, S.; Zhuang, Q.; Li, X.; Wu, P.; Han, Z. *Macromolecules* **2005**, *38*, 9873. (d) Wang, S.; Chen, Y.; Zhuang, Q.; Li, X.; Wu, P.; Han, Z. *Macromol. Chem. Phys.* **2006**, *207*, 2336.
(6) Bai, S. J.; Wu, C. C.; Dang, T. D.; Arnold, F. E.; Sakaran, B. *Appl. Phys. Lett.* **2004**, *84*, 1656.
(7) Dotrong, M.; Mehta, R.; Balchin, G. A.; Tomlinson, R. C.; Sinsky, M.; Lee, C. Y.-C.; Evers, R. C. *J. Polym. Sci., Part A: Polym Chem.* **1993**, *31*, 723.
(8) See for instance: (a) Lee, J.-I.; Kang, I.-N.; Hwang, D.-H.; Shim, H.-K.; Jeoung, S. C.; Kim, D. *Chem. Mater.* **1996**, *8*, 1925. (b) Zhang, X.; Kale, D. M.; Jenekhe, S. A. *Macromolecules* **2002**, *35*, 382.
(9) See for instance: (a) Burn, P. L.; Holmes, A. B.; Kraft, A.; Bradley, D. D. C.; Brown, A. R.; Friend, R. H.; Gymer, R. W. *Nature* **1992**, *356*, 47. (b) Klärner, G.; Davey, M. H.; Chen, W.-D.; Scott, J. C.; Miller, R. D. *Adv. Mater.* **1998**, *10*, 993. (c) Klärner, G.; Lee, J.-I.; Davey, M. H.; Miller, R. D. *Adv. Mater.* **1999**, *11*, 115. (d) Liu, M. S.; Luo, J.; Jen, A. K. Y. *Chem. Mater.* **2003**, *15*, 3496. (e) Vamvounis, G.; Holdcroft, S. *Adv. Mater.* **2004**, *16*, 716. (f) Vamvounis, G.; Schulz, G. L.; Holdcroft, S. *Macromolecules* **2004**, *37*, 8897. (g) Luo, J.; Peng, J.; Cao, Y.; Hou, Q. *Appl. Phys. Lett.* **2005**, *87*, 261103.
(10) (a) Chen, X. L.; Jenekhe, S. A. *Macromolecules* **1996**, *29*, 6189. (b) Chen, X. L.; Jenekhe, S. A. *Appl. Phys. Lett.* **1997**, *70*, 487. (c) Chen, X. L.; Jenekhe, S. A. *Synth. Met.* **1997**, *85*, 1431.

10.1021/cm0621500 CCC: $37.00
Published on Web 01/26/2007

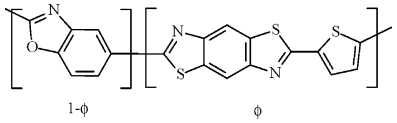

Figure 1. Schematic chemical structure of ABPBO-PBZTT.

copolymers ABPBO-PBZTT shown in Figure 1 and ABPBO/PBZTT blends consisting of ABPBO (when $\phi = 0$) and poly(2,5-thienyl benzobisthiazole) (PBZTT; when $\phi = 1$) have been prepared to explore the effects of structural variation on optical properties. It is anticipated that PBZTT will have a narrower band gap than PBZT as the result of a weaker steric hindrance between the electron-rich thiophene ring and the electron-deficient benzobisothiazole heterocycle. Therefore, copolymers or blends with a larger ΔE_g can be formed by ABPBO and PBZTT to achieve color tunable materials over a wider wavelength range. More importantly, a comprehensive understanding about different exciton migration and trapping mechanisms will be provided and correlated with the local morphology to interpret the photophysical properties of these systems.

Experimental Section

Materials and Synthesis. The synthesis and purification methods for preparing ABPBO, PBZTT, and their copolymers are similar to those for other polybenzazoles.[4,5,7,11] 3-Amino-4-hydroxybenzoic acid hydrochloride (AHBAH)[11] and 2,5-diamino-1,4-benzenedithiol dihydrochloride (DABDT)[3b] were prepared according to previous literature and recrystallized in dilute hydrochloric acid. 2,5-Thiophene diacid (TDA) and methanesulfonic acid (MSA) were purchased from Nanjing Longxi Chemical Co. and Aldrich Chemical Co., respectively, and used as received. A typical synthesis procedure is given as below for ABPBO-PBZTT with a composition of PBZTT (ϕ in Figure 1) of 30%, that is, CO30, and 2.65 g (14 mmol) of AHBAH and 1.47 g (6 mmol) DABDT were was dissolved in 8.30 g of deaerated polyphosphoric acid (PPA) with an equivalent P_2O_5 content of 80%. The reaction vessel was purged with argon. After dehydrochlorination at 80 °C under vacuum, the reaction vessel was cooled to 50 °C before 1.03 g (6 mmol) of TDA was added together with 7.92 g of fresh P_2O_5. The reaction temperature was gradually raised to 90 °C for 6 h, then to 140 °C for 10 h, and finally to 180 °C and held for 12 h. The molar ratio of DABDT/TDA was 1:1, and the molar ratios of AHBAH/DABDT varying from 99:1 to 60:40 were used to achieve copolymers with the PBZTT compositions of 1−40%.

The highly viscous polymerization solution in PPA was precipitated in water and purified by extracting PPA with water for 2−3 days. The polymer was dried at 60 °C in a vacuum oven. Thin films of ABPBO-PBZTT copolymers and ABPBO/PBZTT blends were prepared by spin coating of their solutions in $AlCl_3$/nitromethane with a polymer concentration of ~3 wt % onto silica substrates and vacuum-dried at 80 °C for 12 h after complete decomplexation in deionized water.[12] The molecular structure of the copolymers was established by Fourier transform infrared (FTIR), ^{1}H NMR, and elemental analysis. The results for CO30 are given below as an example. ^{1}H NMR (500 MHz, $AlCl_3/CD_3NO_2$, ppm): δ 9.4 (7H), 9.0−9.2 (20H), 8.7 (6H). FTIR (free-standing film, cm^{-1}): 1622, 1558, 1524, 1460, 1428, 1402, 1310, 1262, 1196, 1120, 1028, 896, 864, 811, 717. Anal. Calcd for $[(C_7H_3NO)_{0.7}-(C_{12}H_4N_2S_3)_{0.3}]_n$: C, 62.37%; H, 2.03%; N, 11.12%. Found: C, 60.04%; H, 2.28%; N, 10.53%. The ^{1}H NMR resonances and FTIR bands of the other copolymers are identical to those of CO30 and are a combination of those of their two parent polymers. The carbon contents measured by elemental analysis are in good agreement with the average values using the two experimental values for the pure components, that is, ABPBO and PBZTT, in the copolymers.

Measurements. Intrinsic viscosities [η] of all the polymers were measured in MSA at 30.0 ± 0.2 °C by using a modified device based on an Ubbelohde capillary viscometer. Thermogravimetric analysis (TGA) was done using a DuPont model 951 thermal analyst, and the data were collected in flowing nitrogen at a heating rate of 10 °C/min. FTIR spectra were taken at room temperature using a Nicolet Magna-IR 550 FTIR spectrometer. The ^{1}H NMR spectra of the polymer solutions in CD_3NO_2 were obtained at 500 MHz using a Bruker DMX-500 instrument. Optical absorption spectra of thin films and polymer solutions were obtained with Varian Cary 500 UV−vis−near-IR spectrophotometers. Photoluminescence (PL) spectra of polymer solutions and films were recorded on an RF-5301 fluorescence spectrophotometer and an Edinburgh fluorescence spectrophotometer at room temperature, respectively.

Results and Discussion

The copolymers with the PBZTT molar compositions of 1, 5, 10, 20, 30, and 40% are named as CO1, 5, 10, 20, 30, and 40, respectively. It must be noted that the real chemical structure of the copolymers could be more complicated than the scheme shown in Figure 1. Particularly when the feed composition ϕ is low, the possibility is statistically high for AHBAH to react with DABDT and TDA on both sides to prohibit the growth of the PBZTT block size. Nevertheless, one single discrete repeating unit for polythiophene or polybenzobisthiazole buried in ABPBO blocks cannot be a low band gap trapping site. The molar composition of PBZTT is therefore only an apparent value in later discussions.

The intrinsic viscosities [η] for ABPBO, CO1-40, and PBZTT, in MSA at 30.0 ± 0.2 °C, are 14.4, 8.0, 6.0, 6.2, 5.6, 5.0, 2.6, and 5.0 $dL\cdot g^{-1}$, respectively. The weight-average molecular weight M_w of ABPBO can be calculated to be 1.05×10^5 $g\cdot mol^{-1}$ using the Mark−Houwink−Sakurada (MHS) equation.[3] Although there are no MHS equations available for the rest of polymers containing PBZTT segments, their molecular weights can be estimated to be above 10 000 $g\cdot mol^{-1}$ when the MHS equation for ABPBO is used. As shown in the TGA thermograms in Figure 2, all the polymers exhibit excellent thermal resistance by the on-set degradation temperatures of 649, 635, 629, 625, 619, 613, 620, and 581 °C and the percentage weight losses at 900 °C of 28, 27, 25, 29, 31, 36, 35, and 44% for ABPBO, CO1-40, and PBZTT, respectively. The results for ABPBO and PBZTT are consistent with the literature,[3,7] and both thermal parameters for copolymers show a rough composition dependence between the value for ABPBO and the value for PBZTT.

The UV absorption and PL emission spectra of ABPBO, PBZTT, and their copolymers in MSA dilute solutions (0.000 48 $g\cdot dL^{-1}$) and thin films are shown in Figure 3.

(11) Chow, A. W.; Bitler, S. P.; Penwell, P. E.; Osborne, D. J.; Wolfe, J. F. *Macromolecules* **1989**, *22*, 3514.
(12) Jenekhe, S. A.; Johnson, P. O.; Agrawal, A. K. *Macromolecules* **1989**, *22*, 3216.

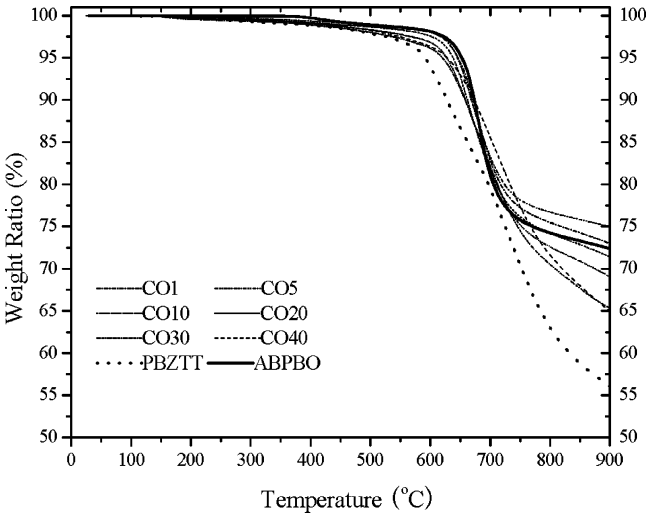

Figure 2. TGA thermograms of ABPBO, PBZTT, and their copolymers heated in nitrogen.

Compared to those of solutions, the absorption spectra of polymer films are less resolved with broadened bandwidth because of interchain interaction. Because of a lower electron cloud density and a shorter effective conjugation length, the absorption band of the ABPBO film appears in a higher-energy range with the maxima at 338 and 355 nm in contrast with that of PBZTT film having maxima at 485 and 518 nm. The dilute solutions' absorption maxima are 493 and 523 nm for PBZTT and 359 and 376 nm for ABPBO, respectively. In copolymers, two absorption shoulders appear in a low-energy range and can be ascribed to PBZTT segments incorporated into ABPBO. They grow progressively with increasing PBZTT composition, and the absorption edge (λ_{onset}) red shifts as shown in Figure 3A. The E_g value determined from λ_{onset} decreases from 3.20 eV for ABPBO to 2.25 eV for PBZTT, which is between ~2.2 eV for polythiophene and 2.34 eV for polybenzobisthiazole.[4c]

For the CO1 dilute solution shown in Figure 3A, the PL emission from PBZTT segments is already comparable to that from ABPBO upon adding only 1% PBZTT. At a higher composition of 5%, emission from ABPBO segments is suppressed significantly, and an identical emission spectrum could be obtained when excited at 406 nm where ABPBO does not absorb. All these phenomena suggest that an efficient intramolecular energy transfer occurs from the higher band gap ABPBO segments to the lower band gap PBZTT segments upon excitation. As summarized in Figure 7A, the emission maximum λ_{em} red shifts from 386 nm for ABPBO to 407 nm for CO1 while their absorption maxima λ_{abs} are identical. With increasing the PBZTT composition further, λ_{em} continues to increase to 514 nm for CO30 and eventually 545 nm for PBZTT, indicating that the effective conjugated length of the emitting species, that is, discrete PBZTT segments, becomes longer and prohibits the coil-like cis conformation of ABPBO segments in the dilute solutions,[11] as depicted in Figure 7B. The resulting Stokes shifts between λ_{em} and λ_{abs} for these copolymers in the dilute solutions except CO1 (31 nm, 0.25 eV) are much higher (76−99 nm, and 0.47−0.68 eV, respectively) than 10 nm (0.085 eV) for ABPBO and 22 nm (0.096 eV) for PBZTT. In agreement with our earlier report on PBO−PBOT

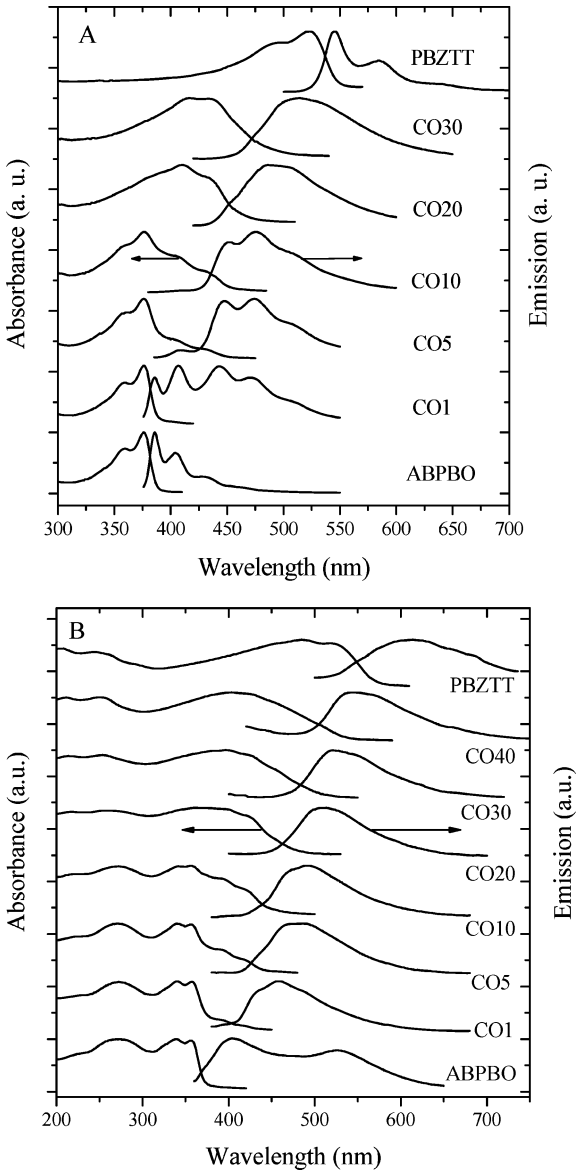

Figure 3. Optical properties of ABPBO, PBZTT, and their copolymers (A) in MSA solutions excited at 493 nm for PBZTT and 376 nm for the rest and (B) in film excited at 485 nm for PBZTT and 357 nm for the rest.

copolymers,[5c] λ_{onset} in absorption spectra (not shown) increases at the same pace as λ_{em}.

Color tuning can be also seen for the polymer films in Figure 3B. The emission maximum is at 604 and 404 nm for PBZTT and ABPBO, respectively. The repeatable emission peak of ABPBO at ~524 nm and the broad and featureless emission spectrum of PBZTT are due to the formation of aggregates.[4a,5a] In comparing emission profiles with those of ABPBO and PBZTT, emission from copolymers clearly emanates from PBZTT segments, and no emission is observed from ABPBO segments despite direct excitation of these segments with a 357 nm light. The emission maximum red shifts from 458 to 480, 491, 511, 524, and eventually 544 nm upon traversing the series CO1 to CO40, indicating that the emitting PBZTT segments become progressively longer with increasing PBZTT composition. Besides the size effect, PBZTT chromophores are spatially confined and isolated to avoid the interchain interaction and the formation of aggregation up to the PBZTT composition of 30%, as evidenced in Figure 7A by the

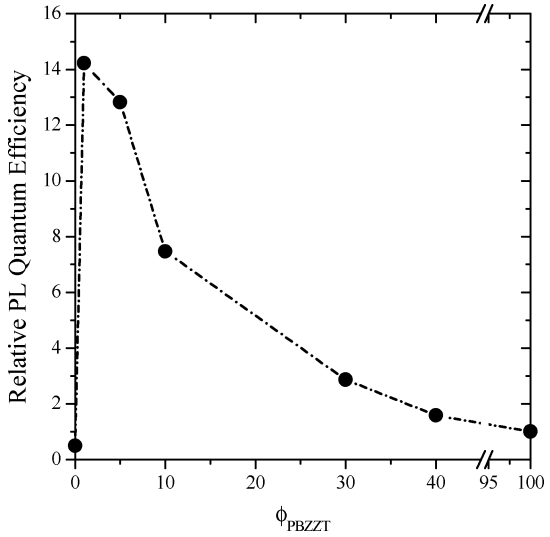

Figure 4. Relative PL quantum efficiency as a function of PBZZT molar composition in copolymers.

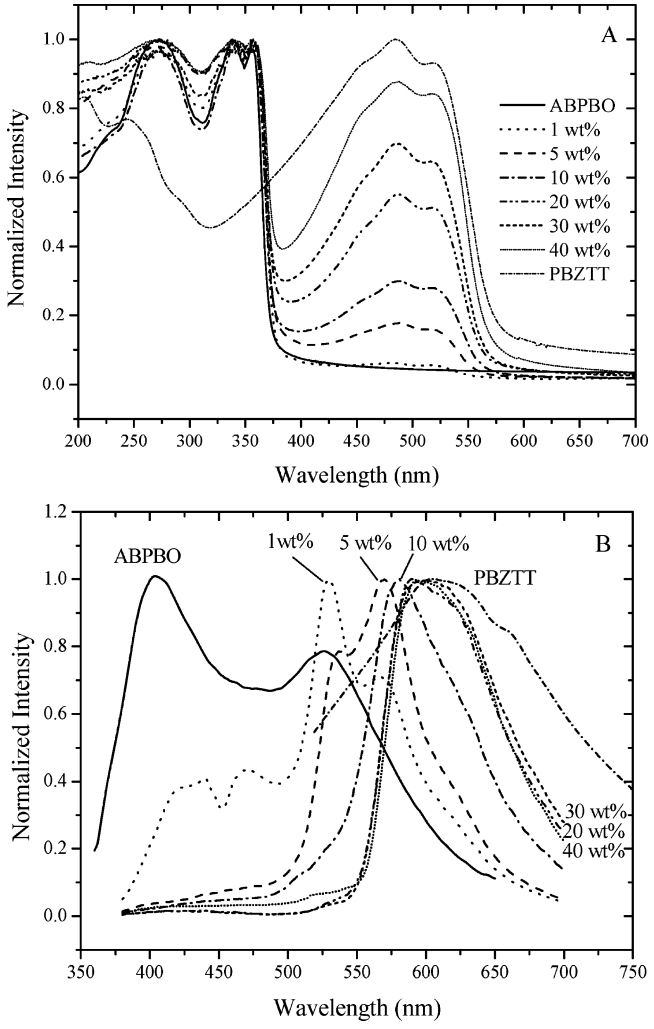

Figure 5. Solid-state optical properties of ABPBO, PBZTT, and their blends with different weight compositions of PBZTT: (A) absorption and (B) emission excited at 485 nm for PBZTT and 357 nm for the rest.

emissive wavelengths similar to those of "single chain" emission in dilute solution. When the composition is higher than 30%, PBZTT segments will inevitably form aggregates to trap excitons and emit as pure PBZTT.

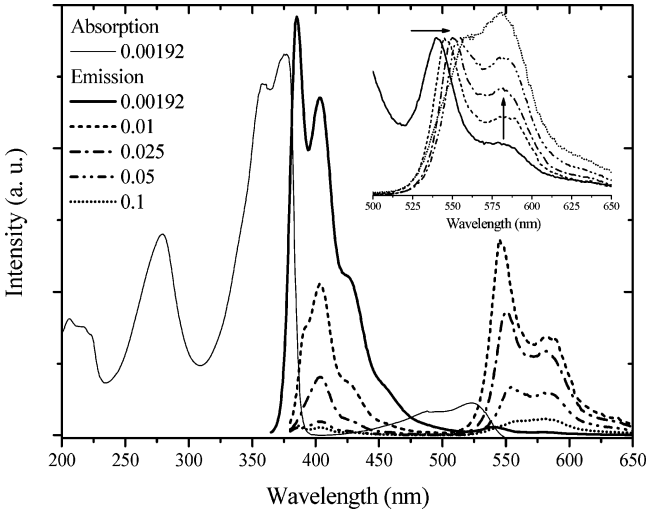

Figure 6. Solution optical properties of an ABPBO/PBZTT blend with 10 wt % PBZTT at various concentrations (in $g \cdot dL^{-1}$). Excitation wavelength: 376 nm. Inset: emission spectra normalized to the peak at around 550 nm.

Figure 4 shows the relative PL quantum efficiencies of ABPBO, PBZTT, and their copolymers obtained by normalizing the integration of PL emission spectra to the value of PBZTT. The relative luminescence efficiency of PBZTT could be enhanced by as much as 14 times compared to pure PBZTT when the composition of PBZTT in copolymer is 1% and it drops with increasing PBZTT composition. As revealed in other copolymer systems consisting of two segments with distinct band gaps[5c,9,10] or conjugated and nonconjugated segments,[4b,5b] the enhanced quantum efficiency for the ABPBO-PBZTT copolymers herein originates from both (1) the spatial confinement effect that can reduce the interchain interaction[4b,5b] and (2) energy transfer that results in increasing the possibility at the low-energy sites for electrons and holes to capture each other, hindering excitons from migrating to ABPBO aggregate quenching sites and reducing self-absorption losses as the emission is red-shifted relative to the absorption edge.[9]

As the solid-state emission of ABPBO overlaps with the absorption spectra of PBZTT demonstrated in Figure 3B, the intermolecular energy transfer system could be prepared by blending these two components according to Förster energy-transfer principle.[8a] Polymer blends of ABPBO and PBZTT with various PBZTT weight fractions of 1−40 wt % (0.43−22.3% in molar composition, correspondingly) have been investigated in comparison with their copolymer counterparts. The absorption spectra of the blends in Figure 5A are a simple superposition of those of ABPBO and PBZTT, suggesting that there is no energy transfer in the ground state.[8] The intensity ratio of these two absorption bands correlates to the mass ratio of PBZTT to ABPBO while the positions of the absorption maxima are invariant of mass ratio.

Figure 5B shows the PL emission spectra of ABPBO, PBZTT, and their blends. The emission spectrum of the blend with 1 wt % PBZTT shows both components. When the PBZTT composition reaches 5 wt %, emission from ABPBO chains is greatly suppressed. For the blend with 10 wt % PBZTT, the maximum emission emanating from PBZTT

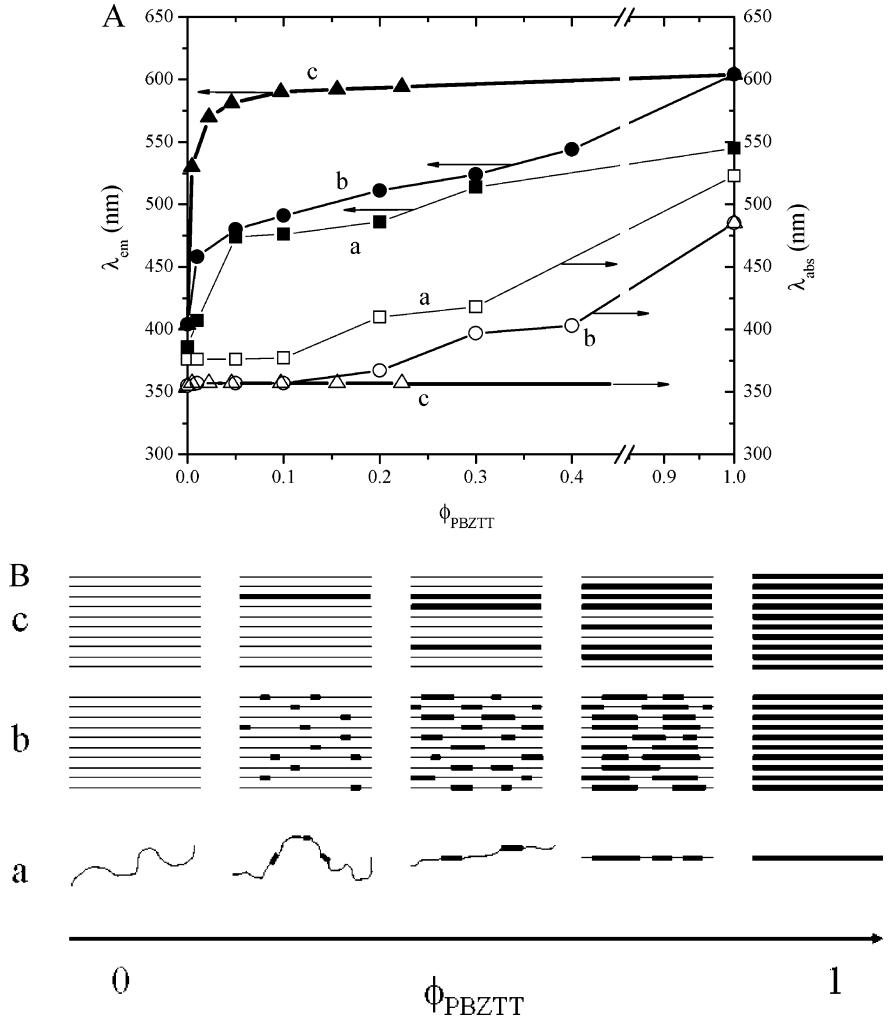

Figure 7. (A) Absorption maximum λ_{abs}, emission maximum λ_{em}, and (B) schematic illustration of the local morphology as a function of PBZTT molar composition ϕ_{PBZTT} for (a) copolymers in solution; (b) copolymers in film; and (c) polymer blends in film.

chains occurs at 580 nm with negligible emission from ABPBO chains though excited at 360 nm, indicating that a fast intermolecular energy transfer occurs from ABPBO to PBZTT in the blends. As shown in Figure 7A, the λ_{em} value of the blends increases rapidly in a small PBZTT molar composition range (0−10%) and levels off to an asymptotic value that is similar to that of PBZTT. It can be interpreted using Figure 7B, in which the discrete PBZTT segments in the copolymers are efficiently dispersed in the ABPBO matrix like solid−solution whereas the PBZTT chains in the blends tend to form aggregates at a lower critical composition because they have a larger size.[4b,10] Only when the PBZTT composition is 1 wt % (0.41% in molar composition in Figure 7A) can the emitting wavelength of 530 nm be close to that of the "single chain" emission of PBZTT. As a result of the composition-dependent exciton confinement effect in the blends, their emission spectra show blue shift and band narrowing relative to pure PBZTT. Similar behavior has also been reported earlier by Chen and Jenekhe on the binary blends of ABPBO-*b*-PBZT-*b*-ABPBO and ABPBO.[10b,c] The quantum efficiencies of the blends in the composition range studied here are only similar to those of their pure components.

The MSA solutions with different polymer concentrations of the ABPBO/PBZTT blend containing 10 wt % PBZTT have been investigated in terms of UV absorption and PL emission spectra, as shown in Figure 6. Similar to their solid counterparts in Figure 5A, the absorption spectra of these solutions have two distinct bands of ABPBO and PBZTT. At 0.001 92 g·dL^{-1}, the emission from ABPBO chains dominates with a very weak emission from PBZTT chains, indicating the intermolecular energy transfer is negligible as the energy transfer rate is inversely proportional to the sixth power of the intermolecular distance.[8a] When the concentration reaches 0.01 g·dL^{-1}, the emission from PBZTT increases while that from ABPBO drops dramatically as a result of self-quenching and enhanced intermolecular energy transfer. In the inset of Figure 6, the emission maximum at 540 nm at 0.001 92 g·dL^{-1} red shifts to 557 nm at 0.1 g·dL^{-1}, and the shoulder around 580 nm grows when the emission spectra were normalized to the peak around 550 nm, indicating the formation of aggregates.[4a,5a]

As discussed together with Figures 3−5 in the previous paragraphs, Figure 7 summarizes the emission and absorption maxima in those cases and supplies a schematic illustration of the composition-dependent supramolecular structures for the copolymers and blends on the basis of the experimental evidence and literature data.[4b,5b,c,8−10] Consequently, the distinct supramolecular structures result in different exciton migration and trapping mechanisms and optical character-

istics. Such correlation between the structure and photophysical properties not only supplies a reasonable basis for exploring the polybenzazole systems in the optoelectronic applications but also can be generalized for other similar host−guest copolymer/blend systems.

Conclusion

In summary, a series of ABPBO-PBZTT statistical, random copolymers have been prepared and characterized. As their parent polymers, ABPBO-PBZTT copolymers exhibit excellent thermal stability with the on-set degradation temperatures ranging from 581 to 649 °C. The ABPBO-PBZTT copolymers, together with ABPBO/PBZTT blends with different PBZTT compositions, demonstrate the spectral modulation and inter- and/or intramolecular energy transfer in both dilute solution and the solid state. The mechanism of exciton migration and trapping differs much in these cases because the local morphology evolves differently with composition. Solid-state copolymers with discrete PBZTT segments resemble a solid-state solution at low PBZTT compositions and exhibit enhanced relative quantum efficiencies as high as 14 times compared to PBZTT. Although there is also efficient interchain energy transfer in the blends, they do not show quantum efficiency enhancement because PBZTT chains are much longer than the PBZTT segments in the copolymers and liable to form aggregates, lower-energy sites, to trap all the excitons.

CM0621500